J|A|C|S
ARTICLES
Published on Web 04/06/2007

Detection of MicroRNAs Using Target-Guided Formation of Conducting Polymer Nanowires in Nanogaps

Yi Fan, Xiantong Chen, Alastair D. Trigg, Chih-hang Tung, Jinming Kong, and Zhiqiang Gao*

Contribution from the Institute of Microelectronics, 11 Science Park Road, Singapore 117685, Republic of Singapore

Received October 19, 2006; E-mail: gaozq@ime.a-star.edu.sg

Abstract: A nanogapped microelectrode-based biosensor array is fabricated for ultrasensitive electrical detection of microRNAs (miRNAs). After peptide nucleic acid (PNA) capture probes were immobilized in nanogaps of a pair of interdigitated microelectrodes and hybridization was performed with their complementary target miRNA, the deposition of conducting polymer nanowires, polyaniline (PAn) nanowires, is carried out by an enzymatically catalyzed method, where the electrostatic interaction between anionic phosphate groups in miRNA and cationic aniline molecules is exploited to guide the formation of the PAn nanowires onto the hybridized target miRNA. The conductance of the deposited PAn nanowires correlates directly to the amount of the hybridized miRNA. Under optimized conditions, the target miRNA can be quantified in a range from 10 fM to 20 pM with a detection limit of 5.0 fM. The biosensor array is applied to the direct detection of miRNA in total RNA extracted from cancer cell lines.

Introduction

MicroRNAs (miRNAs) are a family of non-protein-coding, endogenous, small RNAs. These highly conserved, single-stranded ~22-nucleotide RNAs regulate the expression of genes by binding to the 3′-untranslated regions of mRNAs through a dual mechanism of translational repression and target degradation, but the precise mechanism by which miRNAs silence their target mRNAs remains a subject of research.[1] The interest in miRNAs has increased tremendously in the last 3 years, although the first miRNA was reported in the early 1990s.[2] It is estimated that vertebrate genomes may encode up to 1000 miRNAs, which may regulate up to 30% of the genes.[3,4] Recent studies show that, in addition to their regulatory role in a wide range of metabolic and developmental processes, some miRNAs are directly involved in human cancers, such as leukemia, breast, lung, brain, liver, and colon cancers, and others may function as oncogenes or tumor suppressors.[5] More than 50% of miRNAs are located in cancer-associated genomic regions or in fragile sites.[6] MicroRNAs may play a much more important role in the pathogenesis of human cancer than previously thought and may be clinically important biomarkers for many cancer types.

The extremely small size and similarity among family members of miRNAs have presented challenges for developing ultrasensitive miRNA assays. Northern blot remains the gold standard of miRNA expression profiling.[7] However, there are several technical limitations that prevent researchers from using Northern blot as a routine miRNA expression profiling tool.[7] Earlier attempts to develop ultrasensitive assays for miRNAs were mostly based on optical detections, including a variety of biochemical and chemical ligation-based techniques[8−12] and PCR-based assays.[13−17] For example, Miska and co-workers proposed an array-based miRNA expression profiling procedure, in which miRNAs are ligated to 3′ and 5′ adaptor oligonucleotides followed by RT-PCR.[8] A T4 RNA ligase-based[9] and a RNA-primed, array-based Klenow enzyme assay[10] were also used to couple the 3′ end of miRNA to a fluorophore-tagged nucleotide. Babak et al. proposed a cisplatin-based chemical ligation procedure for miRNAs.[11] Another chemical ligation

(1) Lee, Y.; Ahn, C.; Han, J.; Choi, H.; Kim, J.; Yim, J.; Lee, J.; Provost, P.; Radmark, O.; Kim, S. *Nature* **2003**, *425*, 415−419.
(2) Lee, R. C.; Feinbaum, R. L.; Ambros, V. *Cell* **1993**, *75*, 843−854.
(3) Lewis, B. P.; Burge, C. B.; Bartel, D. P. *Cell* **2005**, *120*, 15−20.
(4) Xie, X.; Lu, J.; Kulbokas, E. J.; Golub, T. R.; Mootha, V.; Lindblad-Toh, K.; Lander, E. S.; Kellis, M. *Nature* **2005**, *434*, 338−345.
(5) Calin, G. A.; Croce, C. M. *Cancer Res.* **2006**, *66*, 7390−7394.
(6) (a) Calin, G. A.; Sevignani, C.; Dan Dumitru, C.; Hyslop, T.; Noch, E.; Yendamuri, S.; Shimizu, M.; Rattan, S.; Bullrich, F.; Negrini, M.; Croce, C. M. *Proc. Natl. Acad. Sci. U.S.A.* **2004**, *101*, 2999−3004. (b) Calin, G. A.; Croce, C. M. *Nat. Rev. Cancer* **2006**, *6*, 857−866.
(7) Draghici, S.; Khatri, P.; Eklund, A. C.; Szallasi, Z. *Trends Genet.* **2006**, *22*, 101−109.
(8) Miska, E. A.; Alvarez-Saavedra, E.; Townsend, M.; Yoshii, A.; Sestan, N.; Rakic, P.; Constantine-Paton, M.; Horvitz, H. R. *Genome Biol.* **2004**, *5*, R68.
(9) Thomson, J. M.; Parker, J.; Perou, C. M.; Hammond, S. M. *Nat. Methods* **2004**, *1*, 47−53.
(10) Nelson, P. T.; Baldwin, D. A.; Scearce, L. M.; Oberholtzer, J. C.; Tobias, J. W.; Mourelatos, Z. *Nat. Methods* **2004**, *1*, 155−161.
(11) Babak, T.; Zhang, W.; Morris, Q.; Blencowe, B. J.; Hughes, T. R. *RNA* **2004**, *10*, 1813−1819.
(12) Gao, Z. Q.; Yang, Z. C. *Anal. Chem.* **2006**, *78*, 1470−1477.
(13) Krichevsky, A. M.; King, K. S.; Donahue, C. P.; Khrapko, K.; Kosik, K. S. *RNA* **2003**, *9*, 1274−1281.
(14) Liu, C. G.; Calin, G. A.; Meloon, B.; Gamliel, N.; Sevignani, C.; Ferracin, M.; Dumitru, C. D.; Shimizu, M.; Zupo, S.; Dono, M.; Alder, H.; Bullrich, F.; Negrini, M.; Croce, C. M. *Proc. Natl. Acad. Sci. U.S.A.* **2004**, *101*, 9740−9744.
(15) Neely, L. A.; Patel, S.; Garver, J.; Gallo, M.; Hackett, M.; Mclaughlin, S.; Nadel, M.; Harris, J.; Gullans, S.; Rooke, J. *Nat. Methods* **2006**, *3*, 41−46.

procedure at the 3′ end was developed by Gao and Yang.[12] However, poor reliability and differential ligation efficiencies may compromise the quality of the data, and the sensitivity of these assays is not always satisfactory.

As the number of identified miRNA increases, microarrays appear to be an ideal method for profiling in a highly efficient parallel fashion for a large number of miRNAs in a single run. However, microarrays have encountered difficulties in reliably amplifying miRNAs without bias. Also, due to the extremely short nature of miRNAs, there is very little room to fine-tune the hybridization conditions for all miRNAs, which significantly discounts the sensitivity and specificity of microarrays.[13,14] The use of locked nucleic acid probes allowed optimization of the hybridization conditions suitable for all miRNAs, producing an improved microarray platform that offered single base mismatch (SBM) discrimination capability with a detection limit of 500 fM.[15]

To further enhance the sensitivity of miRNA assay, several quantitative real-time PCR (qRT-PCR) approaches for the simultaneous amplification and quantification of miRNAs have been developed recently.[16,17] In each of these approaches, the miRNAs were first lengthened to generate extended sequences suitable for subsequent PCR amplifications. It combined the exceptional amplification power of PCR with quantitative detection of the amplified products in real time during each reaction cycle. Despite the many advantages, a number of challenges need to be addressed in qRT-PCR assays. One major constraint is their limited capacity for multiplexing.[16,17] Running too many replicates as single reactions for a panel of miRNAs is not cost-effective and not feasible for small or rare samples.

Electrical methods, on the other hand, are more advantageous than optical methods because electrical detections often directly (label-free or non-labeling) transduce nucleic acid hybridization events into useful electrical signals such as capacitance[18] and conductance.[19,20] Because of the inherent superiorities of electrical transduction methods, such as excellent compatibility with advanced semiconductor technology, miniaturization, and low cost, nucleic acid biosensors based on electrical detection are able to provide high performance at low-cost with a simple miniaturized readout, and thus are exempt from the problems encountered in the optical detection systems. The detection can be tailored to be extremely sensitive with high multiplexing capability. In addition, combining the unique electronic properties of nanoscale materials, electrical detection systems offer excellent prospects for designing nucleic acid detection devices.

A good example is the use of metal nanoparticles, such as gold nanoparticles, as labels for sensitive electronic transduction of different biomolecular recognition events, following the milestone discovery of several interesting physiochemical properties of oligonucleotide-functionalized gold nanoparticles by Mirkin and co-workers,[21] in which gold nanoparticles were used to bridge a gap between two microband electrodes.[22] A simple detection of a conductance change resulted in a detection limit of 500 fM.[22] Later, the same group demonstrated the superiority of the oligonucleotide-functionalized gold nanoparticles in a number of bioassays.[23−30] Worth mentioning here is the bio-barcode technology. It offers PCR-like sensitivity for both DNA and proteins.[28−30] At the cost of sensitivity, Diessel proposed a modified version of the gold nanoparticle method by introducing online continuously monitoring the autometallographic enhancement process, eliminating the need for multistep enhancement and all of the washing, drying, and measurement cycles in between.[31] Nonetheless, the eventual acceptance of electrical detection techniques will depend on how these techniques compare with the current gold standards, that is, PCR and ELISA, in terms of simplicity, sensitivity, specificity, reliability, and portability.

Unfortunately, the gold nanoparticle-based assays have rather limited applications in miRNA analysis, again, because of the inability for much smaller gold nanoparticle−detection probe conjugates to bind on such small miRNA templates. In view of the many attractive features of direct electrical detections, some fundamental changes could in principle result in a much simpler and more robust system for both long and short nucleic acids, to bring the electrical biosensors one step closer to the market. One possible approach would be to eliminate the second hybridization process with the gold nanoparticle−detection probe conjugates, and consequently replace the gold nanoparticle-initiated silver enhancement by a highly specific one-step in situ amplification process, in which the amplifier is directly associated to the target nucleic acid, and miRNA in particular. Here, we report the development of a simplified and sensitive electrical biosensor array, based on the hybridized miRNA-guided in situ formation of PAn nanowires. The association of PAn with the hybridized miRNA molecules leads to the formation of an electrically conducting nanowire network in the gaps, significantly enhances the conductance, and directly signals the presence of target miRNA in the sample solution. Nucleic acid-guided depositions of conducting nanoparticles[32] and nanowires[33,34] have been reported recently. Leveraging on enzymatic polymerization methods, which provide mild and controllable reaction conditions and make possible the use of delicate biomolecules as templates, conducting polymers have also been fabricated along oligonucleotides and λ-DNA to form nanowires,[33,34] where the phosphate groups in nucleic acid

(16) Chen, C.; Ridzon, D. A.; Broomer, A. J.; Zhou, Z.; Lee, D. H.; Nguyen, J. T.; Barbisin, M.; Xu, N. L.; Mahuvakar, V. R.; Andersen, M. R.; Lao, K. Q.; Livak, K. J.; Guegler, K. J. *Nucleic Acids Res.* **2005**, *33*, e179.
(17) Raymond, C. K.; Roberts, B. S.; Garrett-Engele, P.; Lim, L. P.; Johnson, J. M. *RNA* **2005**, *11*, 1737−1744.
(18) Moreno-Hagelsieb, L.; Lobert, P. E.; Pampin, R.; Bourgeois, D.; Remacle, J.; Flandre, D. *Sens. Actuators, B* **2004**, *98*, 269−274.
(19) Macanovic, A.; Marquette, C.; Polychronakos, C.; Lawrence, M. F. *Nucleic Acids Res.* **2004**, *32*, e20.
(20) Iqbal, S. M.; Balasundaram, G.; Ghosh, S.; Bergstrom, D. E.; Bashir, R. *Appl. Phys. Lett.* **2005**, *86*, 153901.
(21) Mirkin, C. A.; Letsinger, R. L.; Mucic, R. C.; Storhoff, J. J. *Nature* **1996**, *382*, 607−609.
(22) Park, S. J.; Taton, T. A.; Mirkin, C. A. *Science* **2002**, *295*, 1503−1506.
(23) Elghanian, R.; Storhoff, J. J.; Mucic, R. C.; Letsinger, R. L.; Mirkin, C. A. *Science* **1997**, *277*, 1078−1081.
(24) Storhoff, J. J.; Elghanian, R.; Mucic, R. C.; Mirkin, C. A.; Letsinger, R. L. *J. Am. Chem. Soc.* **1998**, *120*, 1959−1964.
(25) Taton, T. A.; Mirkin, C. A.; Letsinger, R. L. *Science* **2000**, *289*, 1757−1760.
(26) Taton, T. A.; Lu, G.; Mirkin, C. A. *J. Am. Chem. Soc.* **2001**, *123*, 5164−5165.
(27) Cao, Y. W. C.; Jin, R. C.; Mirkin, C. A. *Science* **2002**, *297*, 1536−1540.
(28) Nam, J. M.; Stoeva, S. I.; Mirkin, C. A. *J. Am. Chem. Soc.* **2004**, *126*, 5932−5933.
(29) Nam, J. M.; Thaxton, C. S.; Mirkin, C. A. *Science* **2003**, *301*, 1884−1886.
(30) Stoeva, S. I.; Lee, J. S.; Thaxton, C. S.; Mirkin, C. A. *Angew. Chem., Int. Ed.* **2006**, *45*, 3303−3306.
(31) Diessel, E.; Grothe, K.; Siebert, H. M.; Warner, B. D.; Burmeister, J. *Biosens. Bioelectron.* **2004**, *19*, 1229−1235.
(32) Torimoto, T.; Yamashita, M.; Kuwabata, S.; Sakata, T.; Mori, H.; Yoneyama, H. *J. Phys. Chem. B* **1999**, *103*, 8799−8803.
(33) Nagarijan, R.; Roy, S.; Kunar, J.; Tripathy, S. K.; Dolukhanyan, T.; Sung, C.; Bruno, F.; Samuelson, L. A. *J. Macromol. Sci., Pure Appl. Chem.* **2001**, *A38*, 1519−1537.
(34) Ma, Y.; Zhang, J.; Zhang, G.; He, H. *J. Am. Chem. Soc.* **2004**, *126*, 7097−7101.

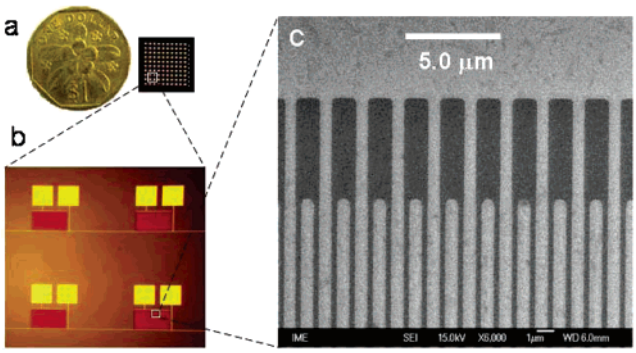

Figure 1. (a) An optical image of 10 × 10 pairs of nanogapped microelectrodes fabricated on a 1.2 × 1.2 cm^2 silicon chip, (b) an optical image of pairs of nanogapped microelectrodes, and (c) a SEM image of the nanogapped microelectrodes.

served as templates to guide the deposition of PAn nanowires. The PAn nanowire formation process is highly specific, occurring only alongside nucleic acid strands. Our electrical miRNA biosensor array is fabricated utilizing this target-guided deposition method. Phosphate groups on the backbone of the hybridized miRNA serve directly as the chemical ligation centers, thus eliminating the second hybridization with the gold nanoparticle−detection probe conjugates, and multiple silver enhancing and washing for signal amplification, enabling a more simplified electrical detection with minimal background and with significantly enhanced sensitivity.

Materials and Methods

Reagents. Amino-terminated PNA capture probes used in this work were custom-made by Eurogentec (Herstal, Belgium) and used as received. Other oligonucleotides were from first Base Pte Ltd. (Singapore). 3-Aminopropyl triethoxysilane (APTES, 99%), aniline (99.5%), and 1,4-phenylenediisothiocyanate (PDITC, 98%) were obtained from Sigma-Aldrich (St. Louis, MO). Horseradish peroxidase (HRP) (200 units/mg) was purchased from Boehringer Mannheim GmbH (Germany). Hydrogen peroxide (31%) was purchased from Santoku BASF (Japan). All other reagents were obtained from Sigma-Aldrich and used without further purification. To minimize the effect of RNases on the stability of miRNAs, all solutions were treated with diethyl pyrocarbonate, and surfaces were decontaminated with RNaseZap (Ambion, TX).

Nanogapped Biosensor Array Fabrication. The biosensor array consisted of 100 pairs of interlocking comb-like microelectrodes (gold 15 nm, titanium 10 nm) with 150−200 fingers, each 700 nm wide and 200 μm long, and with a 300 nm gap. It was fabricated as a 10 × 10 array on a silicon chip with 500 nm coating of SiO_2 by standard photolithography, as depicted in Figure 1. The surface modification of the array was performed according to the method described elsewhere.[35] Briefly, the array was first thoroughly cleaned with chloroform and acetone to remove any possible organic contaminants. After being rinsed with 1.0 M NaOH and a thorough wash with H_2O, it was baked in an oven at 120 °C for 20 min. The silanization of the array was carried out by soaking it in absolute ethanol containing 2% APTES and 1% H_2O (v/v). Next, it was washed with absolute ethanol and allowed to dry under mild nitrogen flow before aging at 120 °C for 20 min. The bifunctional coupling agent PDITC was employed to immobilize the PNA capture probes on the now amino-terminated array. Into a mixture solvent of dimethylformamide and pyridine was added 50 mg of PDITC. Next, the array was allowed to react with the solution for 2 h, followed by washing with dimethylformamide and dichloromethane and subsequent drying under nitrogen flow. The PNA capture probes were dissolved in 0.1% trifluoroacetic acid solution and diluted to a concentration of 1.0 μM with pH 9.0 50 mM sodium carbonate buffer. A 100 μL aliquot of the PNA capture probe solution was spotted onto the array, and the reaction was carried out in a humid chamber at 37 °C for 5 h. Unreacted PNA capture probes were removed by a thorough wash with water and methanol sequentially. Finally, a dimethylformamide solution containing ethanolamine and diisopropylethylamine was used to passivate the biosensor array surface.

Hybridization and Electrical Detection. A schematic illustration of the sensing procedure was depicted in Figure 2. Hybridization was performed in a 10 mM Tris-HCl, 1.0 mM EDTA, and 0.1 M NaCl (TE) buffer at room temperature for 60 min using let-7b as a representative miRNA.[36] After hybridization, the biosensor array was thoroughly rinsed with the hybridization buffer to remove unhybridized miRNA.

Deposition of PAn nanowires after hybridization was accomplished as follows: To a solution of 2.0 mM aniline in pH 4.0 0.10 M NaAc buffer were successively added a 2 μL aliquot of 0.20 mg/mL HRP and stoichiometric amount of H_2O_2. Next, a 200 μL aliquot of the mixture was directly applied to the biosensor array and kept for 30−40 min. The biosensor array was thoroughly washed with blank NaAc buffer solution and water to remove any residual enzyme and aniline monomer, followed by drying under nitrogen flow. A brief (10−20 s) doping was carried out with HCl vapor, and the conductance measurements were performed thereafter under ambient conditions with an Alessi REL-6100 probe station (Cascade Microtech.) and an Advantest R8340A ultrahigh resistance meter (Advantest Corp., Tokyo, Japan). Data were reported as an average of the responses from 20 measurements. All measurements were conducted within the first 30 min after HCl doping.

Results and Discussion

Feasibility Study. PAn is usually prepared in a strong acidic medium via either chemical or electrochemical oxidation, precluding it from being utilized in biosensors due to the harsh conditions required in the process. It was reported that peroxidases, such as HRP, effectively catalyze the polymerization of aniline in the presence of H_2O_2 under very mild conditions.[37−39] However, the products obtained were typically a mixture of different types of polyaniline, including ortho- and para-substituted C−C, C−N bond structures, and the desired head-to-tail structure.[38] The presence of the former greatly diminished the degree of conjugation and hence the electrical properties of the product. Nonetheless, the peroxidase approach has opened new possibilities to engage PAn in a biological system. Recently, Samuelson reported that the use of polyelectrolyte as templates has markedly improved the processibility and electrical properties of PAn through aligning aniline molecules along the polyelectrolyte templates, promoting a more desired para-directed coupling of the aniline molecules. Later, this approach was successfully applied to the fabrication of PAn nanowires using DNA as templates.[34] The above studies provide a good opportunity for the development of an electrical procedure for the detection of miRNA utilizing PAn nanowires as a signal generator for the transduction of miRNA hybridization events.

(35) Liu, B.; Bazan, G. C. *Proc. Natl. Acad. Sci. U.S.A.* **2005**, *102*, 589−593.

(36) (a) Lau, N. C.; Lim, L. P.; Weinstein, E. G.; Bartel, D. P. *Science* **2001**, *294*, 858−862. (b) Griffiths-Jones, S. *Nucleic Acids Res.* **2004**, *32*, D109−D111.

(37) Ryu, K. G.; McEldoon, J. P.; Pokora, A. R.; Cyrus, W.; Dordick, J. S. *Macromolecules* **2000**, *33*, 9542−9547.

(38) Akkara, J. A.; Senecal, K. J.; Kaplan, D. L. *J. Polym. Sci., Part A: Polym. Chem.* **1991**, *29*, 1561−1574.

(39) (a) Liu, W.; Kumar, J.; Tripathy, S. K.; Senecal, K. J.; Samuelson, L. *J. Am. Chem. Soc.* **1999**, *121*, 71−78. (b) Nagarajan, R.; Liu, W.; Kumar, J.; Tripathy, S. K.; Brono, F. F.; Samuelson, L. A. *Macromolecules* **2001**, *34*, 3921−3927.

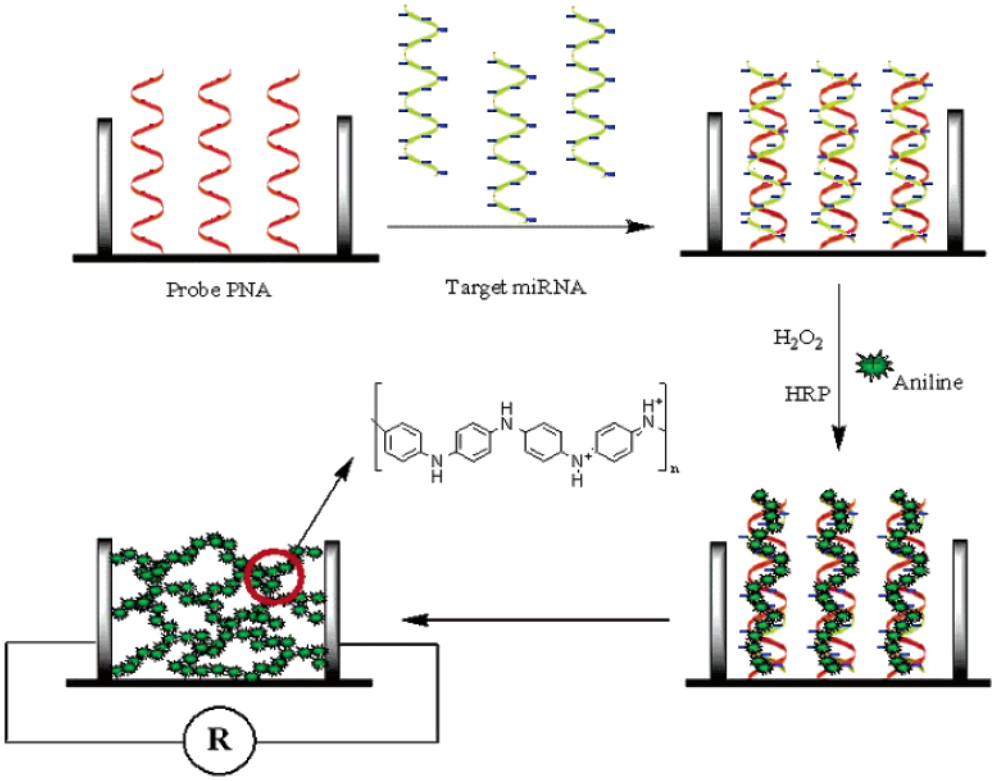

Figure 2. Schematic illustration of the sensing mechanism.

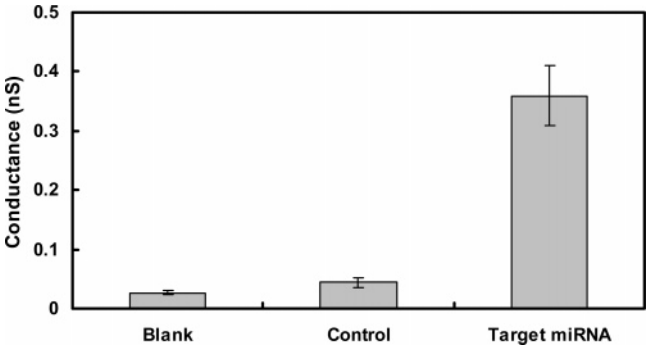

Figure 3. Electrical response of a blank (PNA-modified array without any treatment), a control, and a biosensor array. 2.0 pM of target and noncomplementary miRNAs were used for hybridization. PAn nanowire deposition: 40 min in pH 4.0 NaAc buffer containing 2.0 mM H_2O_2, 2.0 mM aniline, and 1.0 μg/mL HRP.

To demonstrate this concept, we first evaluated the response of the biosensor array with 2.0 pM target miRNA perfectly complementary to the PNA capture probes. For comparison, a control sample was also tested by applying a noncomplementary miRNA for hybridization and then followed with the same procedure as that for the complementary miRNA. As illustrated in Figure 2, PAn deposition was performed using the hybridized miRNA strands as templates. It is expected that the hybridization of the target miRNA to the PNA capture probes resulted in a negatively charged surface originated from the phosphate groups on the miRNA backbone. When the hybridized biosensor array is incubated in the mixture of aniline/HRP/H_2O_2 at pH 4.0, the protonated aniline molecules ($pK_a = 4.6$)[40] are concentrated and aligned around the hybridized miRNA strands through electrostatic interaction between the protonated aniline molecules and phosphates in the miRNA. This high proton concentration around the miRNA provides a local environment of high acidity that permits polymerization of aniline in a much less acidic medium than that in conventional electrochemical and chemical approaches, and facilitates a predominantly head-to-tail coupling and deters parasitic branching during the polymerization, offering the much desired structure for high conductance. The thus formed PAn/miRNA complex in which PAn wraps around the miRNA template (PAn nanowires) is utilized for miRNA sensing. For the complementary miRNA sample, the obvious increase in conductance of the nanogaps with PAn nanowires deposited could not be immediately obtained because the conductance of the as-prepared PAn nanowires is very low.[39] After a simple doping treatment with HCl vapor for 10−20 s, the conductance was measured again, and the results are depicted in Figure 3. A sizable increase in conductance was found for the complementary miRNA, whereas only a slight increase was observed for the control sample when compared to a blank biosensor array (PNA functionalized biosensor arrays without undergoing miRNA hybridization, PAn nanowire deposition, and doping). This clearly demonstrates that the formation of PAn nanowires in the nanogaps is guided by the hybridized miRNA molecules, and the resulted PAn nanowire network bridges the gaps, producing a measurable conductance change. The result of the control sample implies that the non-hybridization-related signal of this biosensor array is extremely low, which facilitates the detection of miRNA at ultralow concentrations. This may be attributed to the use of PNA other than conventional anionic oligonucleotides as the capture probes because, on one hand, PNA has higher affinity toward target miRNA,[41] which can suppress the occurrence of unspecific

(40) Lide, D. R. *Handbook of Chemistry and Physics*, 68th ed.; CRC Press: Boca, Raton, FL, 1993; pp D159−161.

(41) Fortina, P.; Kricka, L. J.; Surrey, S.; Grodzinski, P. *Trends Biotechnol.* **2005**, *23*, 168−173.

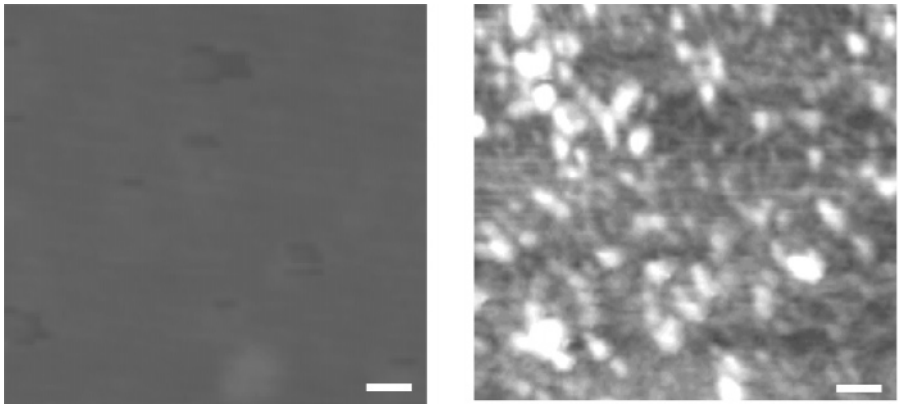

Figure 4. AFM images of a control (left) and a biosensor (right) after hybridization and PAn nanowire deposition. The images were taken from the big gaps at the end of the biosensor to avoid complications caused by the metal fingers. The scale bar is 20 nm.

capture probe-target binding, and, on the other hand, its neutral *N*-(2-aminoethyl)-glycine backbone can prevent the undesired adsorption of aniline monomer, which remarkably reduces the background noise.

The conductance obtained at the biosensor array hybridized to the lowest detectable concentration of 5.0 fM target miRNA was 0.11 nS (conductivity 3.5×10^{-6} S cm^{-1}), which is at the same level as that for DNA−polyaniline pellets[33] and is about 1 order of magnitude lower than that of polyaniline nanowires deposited by using λ-DNA as templates.[34] This could be due to the presence of discontinuous areas in the PAn network in the nanogaps and to the agglomeration of the PAn/miRNA complex strands occurred during deposition.[33]

Atomic force microscopic (AFM) characterization was then performed for the biosensor arrays exposed to the control and to the complementary miRNA samples. The images are shown in Figure 4. It is seen that the control array shows no visible change, while after PAn nanowire deposition, the biosensor array hybridized with the complementary miRNA was obviously roughened by the presence of the PAn nanowire network consisting of overlapped nanowires. Besides, some polyaniline dots and short rods also appeared, which were supposed to be the agglomeration of the short nanowires. The morphology of the PAn deposited is somewhat different from the wire-like polymer found in using aligned long DNA strands as templates for polymerization.[33,38] One possible reason may be that the target miRNA used here is relatively short with only 22 nucleotides (estimated length 7−8 nm) and randomly spreads out in the nanogap. Another possible reason may be that the overwound polymorph and agglomeration of the PAn nanowires occurred with the concomitant shielding of the negative charges on the miRNA template with the proceeding of the PAn formation on it, reducing the electrostatic repulsion between adjacent miRNA strands.[33] Therefore, the deposited PAn was likely to take on an uneven net-like configuration other than independent wires with clear boundaries. Fortunately, agglomeration is actually a desirable feature in developing an electrical detection procedure with the nanogapped electrodes because it greatly facilities the bridging of the nanogaps, making it possible to read electrical signal with high sensitivity.

Optimization. The target-guided formation of PAn nanowires is highly dependent on the electrostatic interaction between cationic aniline monomers and anionic phosphate groups in miRNA; therefore, an acidic buffer solution at pH 4.0 was selected for PAn deposition because it is the most optimal acidity to provide adequate protonation of aniline and thus strong enough electrostatic interaction between aniline and the phosphate groups and also maintains sufficient activity of HRP.[34] Besides, this relatively low pH is found to favor the generation of continuous PAn nanowires other than insulating PAn nanoparticles.[38] To maximize the biosensor performance, the influence of aniline, HRP, and the deposition time on the conductance of the resulting PAn were then thoroughly investigated.

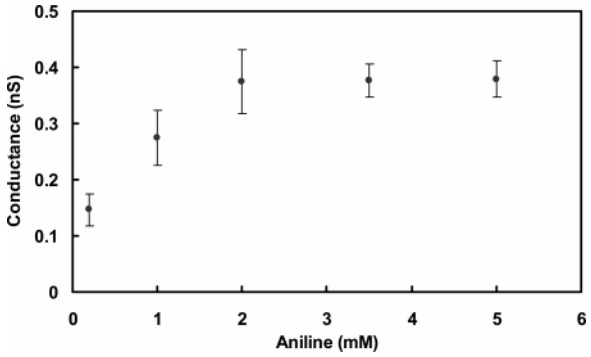

Figure 5. The dependence of conductance of 2.0 pM of target miRNA on aniline concentration. Other conditions are as for Figure 3.

The effect of aniline was first studied by varying the aniline concentration in the mixture solution from 0.50 to 5.0 mM while keeping the HRP concentration and the deposition time unchanged. It has been pointed out in previous studies that a stoichiometric amount of H_2O_2 to aniline should be present in the solution;[38,39] the H_2O_2 concentration was therefore adjusted accordingly in this study. As illustrated in Figure 5, as the aniline concentration increased from 0.50 to 5.0 mM, the conductance of PAn nanowires formed in the nanogaps first increased and then attained a steady value at 2.0 mM. It is known that the rate of enzyme-catalyzed reaction increases with increasing substrate concentration until the substrate concentration is high enough to saturate the enzyme. 2.0 mM of aniline was therefore selected to perform PAn nanowire deposition, which was also high enough to facilitate the longer polymer chain growth and avoid short chain segments formation.[39]

The optimization of HRP concentration was carried out in the range of 0.10−2.5 μg/mL. The results are depicted in Figure 6. The conductance of the PAn nanowire increased with increasing HRP concentration in the range of 0.10−1.0 μg/mL, and further increase in HRP concentration did not show

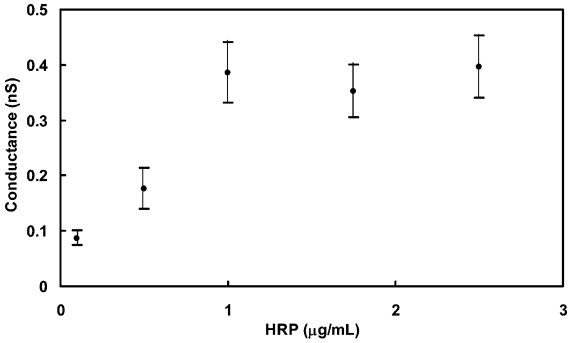

Figure 6. Effect of HRP concentration on conductance of 2.0 pM target miRNA. Other conditions are as for Figure 3.

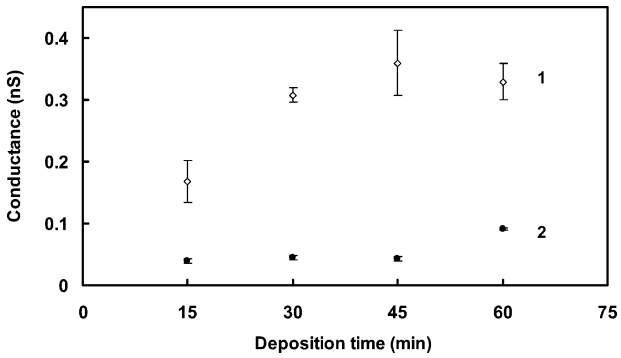

Figure 7. Effect of PAn nanowire deposition time on conductance of the biosensor array hybridized with (1) 2.0 pM complementary and (2) control miRNA. Other conditions are as for Figure 3.

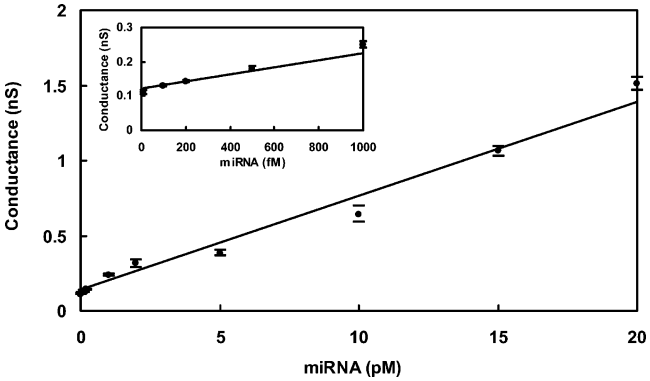

Figure 8. A calibration curve for miRNA. Conditions are as for Figure 3. Inset: The calibration curve at the low concentration end.

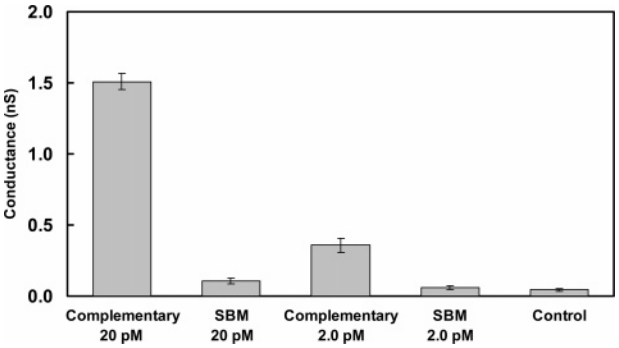

Figure 9. The dependence of conductance of a biosensor hybridized with complementary and SBM miRNA at 2.0 and 20 pM, respectively. Conditions are as for Figure 3.

appreciable changes in conductance. According to the mechanism of enzymatic reactions, the reaction rate scales up proportionally with the enzyme concentration when the substrate concentration is high enough. However, in the case of very high HRP concentration, the polymerization rate is so fast that nontarget-guided aniline polymerization and non-discriminative deposition of PAn are also accelerated and favor the production of highly branched PAn,[38] which results in random deposition of PAn onto the biosensor array and increases the background conductance. This is evidenced by the appearance of a plateau in Figure 6 and a high background obtained for the control sample under high HRP concentrations. Therefore, 1.0 μg/mL of HRP was used for subsequent experiments.

Figure 7 shows the effect of PAn nanowire deposition time on the biosensor array conductance (sensitivity). As expected, the longer is the deposition time, the higher is the conductance. However, an increase of the background noise was noted after 60 min of deposition probably due to the build up of PAn in the gaps from the non-discriminative PAn deposition, similar to that previously observed when there was too much HRP. Therefore, a deposition time of 40 min was selected to ensure the highest sensitivity and the best signal/noise ratio.

Calibration Curve. Utilizing this target-guided deposition of PAn nanowires as the signal amplification method for electrical detection of miRNA, the conductance between the nanogapped electrodes is primarily dependent on the amount (density) of the PAn nanowires formed along the target miRNA strands in the gaps. The more the target miRNA molecules hybridized, the more the PAn nanowires deposited alongside the miRNA strands, thus the higher is the conductance. Because the ratio of the PAn nanowire to target miRNA molecule is fixed at 1:1, the amount of the PNA capture probes immobilized in the gaps and hybridization efficiency determine the amount of target miRNA bound to the biosensor and thereby the amount of PAn nanowires, implying that the target miRNA molecules hybridized in the nanogaps are directly correlated to the conductance, and thus a simple and straightforward linear relationship between the conductance and miRNA concentration can be expected. To construct the calibration curve, 20 measurements were carried out for each concentration to obtain the average of the conductance. Indeed, under optimized conditions, the complementary miRNA can be quantitatively detected in a dynamic range from 10 fM to 20 pM with the regression coefficient R^2 as 0.976, as shown in Figure 8. The detection limit was found to be 5.0 fM. Comparing the gold nanoparticle labeling and silver enhance methods for detection of nucleic acids,[22] the sensitivity of the present assay is 2 orders of magnitude higher, indicating that the PAn nanowires bridge the nanogap much more effectively than gold nanoparticles, greatly enhancing the sensitivity of the biosensor array and thereby lowering the detection limit to femtomolar levels. In practice, this sensitivity of the assay meets the requirements for direct miRNA expression profiling.

Specificity. To evaluate the capability of the proposed method in discriminating SBM in miRNAs, two miRNA samples, let-7b and let-7c (only a single G↔A mismatch between them), were tested at 20 and 2.0 pM at biosensor arrays fully complementary to let-7b, respectively. As shown in Figure 9, the increases in conductance for the SBM sequence let-7c, at 20 and 2.0 pM, were 4.3% and 5.1% of that for let-7b of the same concentration, respectively. That is to say, the detection of the SBM mutations is possible at the biosensor array with a SBM selectivity factor of 20:1, much higher than that of the

optical microarray and most other previously reported methods,[42,43] readily allowing discrimination between the perfectly matched and mismatched miRNAs. The high specificity of the biosensor array suggests that each quantified result represents a specific quantity of a single miRNA member and not the combined quantity of the entire family, offering unique advantages over optical arrays and much broader applications than for miRNA detection.

Application. The ultrasensitive and non-labeling approach proposed in this work is well suited for direct and PCR-free miRNA expression profiling. The applicability of the biosensor in miRNA detection of real world samples was carried out by analyzing let-7b in total RNA extracted from Hela cells and lung cancer cells. Aliquots of the total RNA were diluted with the hybridization buffer and directly applied to the biosensor array. Both samples gave positive conductance changes, and the results were normalized with respect to the total RNA. It was found that the concentration of let-7b in the total RNA extracted from Hela cells and lung cancer cells is $(2.34 \pm 0.29) \times 10^7$ and $(2.53 \pm 0.33) \times 10^7$ copies/μg RNA, respectively. These results are consistent with recently published data of miRNA expression profiling.[44−46] Considering the detection limit of 5.0 fM of the biosensor array, it is possible that a dozen cells are able to provide an adequate amount of total RNA for miRNA detection.[47] The relative standard derivation of the biosensor array was found to be $<15\%$, which provides satisfactory accuracy to distinguish slight miRNA expression differences.

Conclusions

Ultrasensitive detection of miRNA with the target-guided deposition of PAn nanowires as the in situ signal amplification method was demonstrated. This method directly utilized chemical ligation and amplification for signal read-out and thus eliminated the use of labeling probes, which greatly simplifies the detection procedure. In principle, a much lower detection limit could be realized when working with longer target nucleic acids because the bridging of the nanogaps by the PAn nanowires can be realized with fewer long nucleic acid molecules. Multiplex detection can be easily realized by introducing different capture probes onto the biosensor array, which will make it more versatile for various research purposes. Such an in situ amplification strategy may enable the development of a simple, low-cost, and portable electrical array for miRNA expression profiling, opening the door to routine gene expression profiling and molecular diagnostics. Efforts to fabricate such an array for multiplexing and incorporate it into a handheld system are currently underway.

Acknowledgment. We are grateful to IME/A*STAR for their support of our research. We thank Mr. Y. H. Yu for his help in molecular biological experiments.

JA067477G

(42) Rosi, N. L.; Mirkin, C. A. *Chem. Rev.* **2005**, *105*, 1547−1562.
(43) Xie, H.; Zhang, C.; Gao, Z. Q. *Anal. Chem.* **2004**, *76*, 1611−1617.
(44) Nelson, P. T.; Baldwin, D. A.; Scearce, L. M.; Oberholtzer, J. C.; Tobias, J. W.; Mourelatos, Z. *Nat. Methods* **2004**, *1*, 155−161.
(45) Allawi, H. T.; Dahlberg, J. E.; Olson, S.; Lund, E.; Olson, M.; Ma, W. P.; Takova, T.; Neri, B. P.; Lyamichev, V. I. *RNA* **2004**, *10*, 1153−1161.
(46) Barad, O.; Meiri, E.; Avniel, A.; Aharonov, R.; Barsilai, A.; Bentwich, I.; Einav, U.; Gilad, S.; Hurhan, P.; Karov, Y.; Lobenhofer, E. K.; Sharon, E.; Shiboleth, Y. M.; Shtutman, M.; Bentwich, Z.; Einay, P. *Genome Res.* **2004**, *14*, 2486−2494.
(47) Lim, L. P.; Lau, N. C.; Weinstein, E. G.; Abdelhakim, A.; Yekta, S.; Rhoades, M. W.; Burge, C. B.; Bartel, D. P. *Genes Dev.* **2003**, *17*, 991−1008.